The Longevity-Frailty Hypothesis: Evidence from COVID-19 Death Rates in Europe

Levi Altringer*[a], Sammy Zahran*[a,b], and Ashok Prasad[c]

[a]Department of Economics, Colorado State University, Fort Collins, CO
[b]Department of Epidemiology, Colorado School of Public Health, Fort Collins, CO
[c]Department of Chemical and Biological Engineering, Colorado State University, Fort Collins, CO

May 20, 2020

Abstract

The COVID-19 death rate (deaths over population) is strikingly unevenly distributed across Europe. While the risk of death from COVID-19 increases non-linearly in age, within-age-group variation in COVID-19 death rates across countries suggests that age structure alone cannot account for observed differences in COVID-19 mortality risk. Age-related conditions that render the elderly less resistant to health shocks are non-obviously positively related to the survival environment. More favorable survival environments promote longevity and the accumulation of health frailty among the elderly while less favorable survival environments induce a mortality selection process that results in a lower amount of accumulated health frailty. To explain observed differences in COVID-19 mortality across the countries of Europe, we employ cross-national variation in pre-existing age-specific probabilities of death to identify heterogeneous survival environments and produce model-generated measures of accumulated health frailty. We find a strong positive relationship between our model-generated measures of accumulated health frailty and COVID-19 death rates ($r = 0.772$, $p < .001$) across the countries of Europe, a result that is robust to statistical control for the timing and strength of epidemic seeding from exported cases, the capacity of healthcare systems to manage and survive infected persons, as well as the timing and stringency of non-pharmaceutical interventions. Our results oblige the stylized facts that the risk of COVID-19 mortality is nonlinearly increasing in age and that a disproportionate share of deaths are occurring among frail populations in long-term care facilities.

*Corresponding authors: laltrin@colostate.edu and szahran@colostate.edu. We wish to acknowledge helpful feedback from Anders Fremstad, Christopher Keyes, Ryan Levitt, Salvador Lurbe, Sophie McKee, David Mushinski, Christopher Slootmaker, Daniele Tavani, and Peter Zahran.

1 Introduction

The COVID-19 death rate (deaths over population) is strikingly unevenly distributed across Europe. Figure 1 arranges the countries of Europe in descending order by the recorded COVID-19 deaths per million, as of May 1st, 2020. Atop the list are Belgium, Spain, and Italy, with COVID-19 death rates of 665, 525, and 467 deaths per 1 million, respectively.[1] Spain's COVID-19 death rate exceeds similarly developed economies of Germany (81 per million) and Austria (65 per million) by more than a factor of 6. Few, if any, epidemiological indicators distinguish the countries of Europe by such an extent.

Figure 1: COVID-19 Deaths per 1 Million Persons Across European Countries (as of May 1st, 2020)

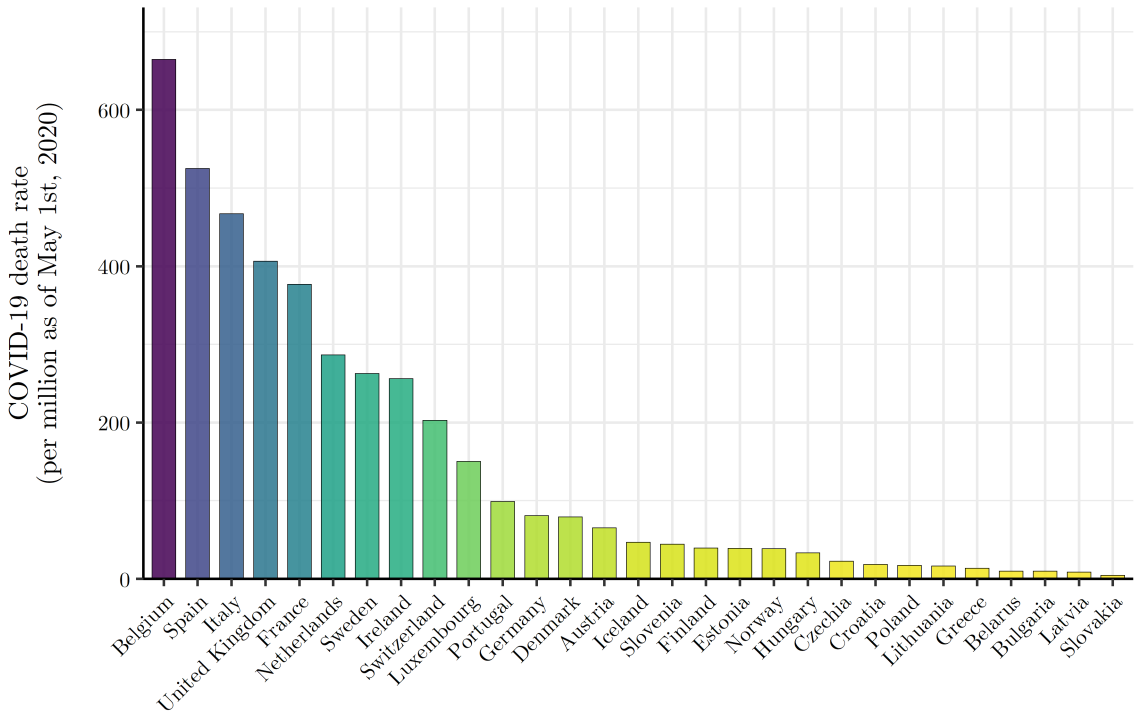

NOTE: COVID-19 death data by country are from Johns Hopkins Coronavirus Resource Center.

COVID-19 disproportionately afflicts the elderly, especially the elderly with underlying health conditions. This is evidenced by 1) case-fatality ratios (deaths over observed infections) and death rates (deaths over population) that are nonlinearly increasing in age and 2) the disproportionate share of deaths occurring among frail populations around the world (Dowd et al., 2020; Dudel et al., 2020). Consider Figure 2, plotting age-specific COVID-19 death rates (as of May 1st, 2020) for six European countries whose data were available at the time of writing. The size of the points plotted in Figure 2 reflect the share of total reported COVID-19 deaths that can be attributed to each age group within

[1] Belgium's method of reporting COVID-19 deaths includes not only deaths that are confirmed to be virus-related, but also deaths that are suspected of being linked, even if the victim was tested or not.

country. While the risk of death is increasing in reported age intervals, most striking is that much of the cross-national variation observed in Figure 1 is maintained. For instance, Spain's age-specific death rates are roughly 5 times that of Germany's across all age groups. The within-age-group variation in COVID-19 death rates across countries implies that the age structure of the population alone cannot account for observed differences in COVID-19 mortality risk among the countries of Europe.

Across the six countries in Figure 2, persons 70 years of age and older account for more than 80 percent of all reported COVID-19 deaths. Frailty is a term used to capture a range of age-related conditions that render the elderly less resistant to health shocks (Hoogendijk et al., 2019; Theou et al., 2018; Vetrano et al., 2018; Denfeld et al., 2017). The risk and accumulation of frailty in a society is non-obviously positively related to the survival environment (Vogt & Missov, 2017; Vaupel et al., 1979). Consider two similarly economically developed countries with varying survival to age of 75, the accepted standard for premature death. Suppose that one country has high and the other low risk of premature death from all causes. Persons surviving to 75 in the high-risk all-cause mortality country are more positively selected on the underlying ability to persist than counterparts in the low-risk all-cause mortality country. Given mortality selection, elderly persons over the age of 75 in the high-risk country are also more likely to withstand adverse health shocks than similarly aged persons in the low-risk country because they are different on the risk of frailty.

Figure 2: Age-Specific COVID-19 Deaths per 1 Million Persons (as of May 1st, 2020) Across Select European Countries

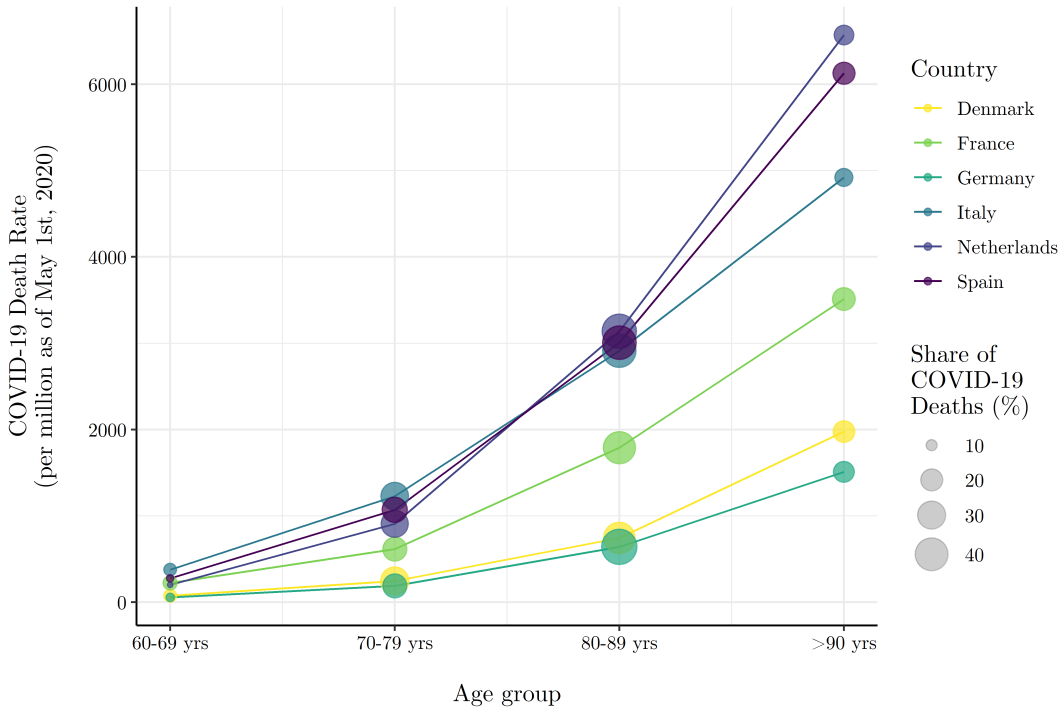

NOTE: COVID-19 death data by age, sex and, country are from National Institute for Demographic Studies (INED).

In this paper we develop measures of accumulated health frailty in an attempt to explain observed differences in COVID-19 mortality across the countries of Europe. We begin by developing a simple model of longevity and accumulated health frailty. Each country begins with an identical underlying distribution of health frailty among the population. Then, heterogeneous survival environments across countries induce a mortality selection process that generates varying amounts of accumulated health frailty in subsequent periods, or old-age. Specifically, more favorable survival environments promote longevity and a larger amount of accumulated health frailty while less favorable survival environments induce a relatively strict mortality selection process that results in a lower amount of accumulated health frailty among the elderly. With respect to an exogenous health shock that disproportionately targets the relatively health frail, like COVID-19, this simple model implies that countries with a more favorable survival environment will have a larger susceptible (health frail) population and, therefore, a higher COVID-19 death rate.

Employing cross-national variation in pre-existing age-specific probabilities of death to identify heterogeneous survival environments, we produce model-generated measures of accumulated health frailty among the countries of Europe. Then, using both pre-existing all-cause mortality rates and our model-generated measures of accumulated health frailty, we show that a more favorable survival environment has a strong positive association with the COVID-19 death rate across the countries of Europe. This result is robust to statistical control for competing theories of COVID-19 prevalence and mortality, including the timing and strength of epidemic seeding from exported cases, the capacity of a healthcare system to manage and survive infected persons, as well as the timing and stringency of non-pharmaceutical interventions, and obliges stylized facts that 1) the risk of COVID-19 mortality is nonlinearly increasing in age and 2) that a disproportionate share of deaths are occurring among frail populations in long-term care facilities.

2 The Longevity-Frailty Hypothesis

2.1 Modeling the Longevity-Frailty Hypothesis

Consider a simple model of survival with two periods, $t = (1, 2)$. In period $t = 1$, a country (j) begins with a representative population of individuals (i) who are each endowed by nature with a level of health frailty (f_i).[2] Health frailty ranges from 0 (least frail) to 1 (most frail) and is assumed to be distributed normally across the population with the imposed restriction that $\Pr[0 \leq f \leq 1] = 1$ since $f \in [0, 1]$.[3]

[2]Health frailty can be thought of as the inverse of a stock of health.

[3]Specifically, the initial normal distribution of health frailty is defined by $\mu = 0.5$ and $\sigma = 0.15$. The assumed distribution of health frailty in period $t = 1$ is inconsequential to the implications of the model so long as the same distribution is

The likelihood that an individual survives to period $t = 2$ is determined by a Bernoulli trial. Specifically, individual i in country j survives to period $t = 2$ with probability $p(f_i; \delta_j)$ or, equivalently, dies in period $t = 1$ with probability $1 - p(f_i; \delta_j)$. The survival probability function $p(f; \delta)$, defined over the domain of health frailty, takes the following functional form

$$p(f; \delta) = 1 - f^{\delta} \tag{1}$$

where $\delta > 1$. Taking the first and second derivative of the survival probability function with respect to health frailty shows that the probability of survival increasingly deteriorates in health frailty

$$\frac{\partial p}{\partial f} = -\delta f^{\delta - 1} < 0 \tag{2}$$

$$\frac{\partial^2 p}{\partial f^2} = -\delta(\delta - 1) f^{\delta - 2} < 0 \tag{3}$$

with certain survival for the least frail—$p(0; \delta) = 1$—and certain death for most frail—$p(1; \delta) = 0$). The exponent δ is a survival environment parameter. For a given level of health frailty in the range $(0, 1)$ a more favorable survival environment increases an individual's likelihood of surviving into old age. Specifically,

$$\frac{\partial p}{\partial \delta} = -\ln(f) f^{\delta} > 0 \tag{4}$$

so that larger values of δ reflect a more favorable survival environment. While we do not explicitly model the determination of δ, the environmental parameter is a function of several factors that contribute to improved life expectancy for all individuals across the health frailty distribution. These factors include, but are not limited to, income, nutrition, public health, vaccination, medical treatments, and social welfare policy (Cutler, Deaton, & Lleras-Muney, 2006).

Given the survival probability function, we can now derive the expected accumulation of health frailty in period $t = 2$. Let N_f^1 denote the number of individuals in period $t = 1$ with health frailty f. Then the expected number of persons with health frailty $f \geq h$ that survive to period $t = 2$ is given by

$$E[N_{f \geq h}^2] = \int_h^1 N_f^1 p(f; \delta) df = \int_h^1 N_f^1 (1 - f^{\delta}) df \tag{5}$$

and the expected number of relatively frail individuals ($f \geq h$) that survive to period $t = 2$ is increasing

assumed for all countries.

in δ

$$\frac{\partial E[N^2_{f\geq h}]}{\partial \delta} = -\int_h^1 N^1_f \ln(f) f^\delta df > 0; \quad h \in (0,1). \tag{6}$$

Thus, this simple model outlines a clear relationship between a country's survival environment (δ) and the expected accumulation of health frailty among the elderly (period $t = 2$).[4] To make this relationship more clear, we simulate a discrete version of the model presented above.

Health frailty is distributed normally in period $t = 1$, as previously discussed, but health frailty is now defined to take on the discrete values $f \in \{0, 0.01, ..., 0.99, 1\}$. This initial distribution of health frailty is displayed in panel (a) of Figure 3 for a representative population of 100,000 individuals. In panel (b) we present six hypothetical survival environments, or countries, whose survival probability functions are shaped according to equation (1) with varying values of δ.

Again, for individual i in country j, a Bernoulli trial is performed where a 0 (dies in period $t = 1$) is drawn with probability $1 - p(f_i; \delta_j)$ and a 1 (survives to period $t = 2$) is drawn with probability $p(f_i; \delta_j)$. For example, an individual with health frailty $f = 0.8$ living in a survival environment characterized by $\delta = 2$ would die in period $t = 1$ with probability $1 - p(0.8; 2) = 1 - [1 - (0.8)^2] = 0.64$ and survive to period $t = 2$ with probability $p(0.8; 2) = 1 - (0.8)^2 = 0.36$. This Bernoulli trial is performed for each of the 100,000 individuals in each country according to their own endowment of health frailty (f_i) and their country's survival environment (δ_j).

Let $f = h = 0.8$ be the definitive health frailty cutoff so that all individuals with $f \geq h = 0.8$ comprise the population of frail individuals.[5] In panel (c) of Figure 3 we plot the distribution of the health frail population in period $t = 2$. The previously derived condition (6), which showed that the expected number of relatively frail individuals surviving to period $t = 2$ is increasing in δ, is now clearly visible. Intuitively, countries with a more favorable survival environment have a larger population of relatively frail individuals. The frail survival rate is presented in panel (d) of Figure 3.

[4] It is important to note that an individual's health frailty is not endogenously determined in this simple model, a point that we return to in the conclusion of our paper. Specifically, a less favorable survival environment may positively contribute to the accumulation of health frailty through "scarring" or "weathering" effects even though the process of mortality selection negatively contributes to accumulated health frailty, or what some refer to as the "culling" effect (Almond & Currie, 2011). A model that incorporates these competing effects would provide a more general theoretical understanding of accumulated health frailty that would be better able to explain within-country variation in health outcomes and/or mortality across groups—e.g. the relatively high COVID-19 death rates observed for African Americans in the US (Yancy, 2020) and the positive association between COVID-19 death risk and multiple deprivation in the UK (Williamson et al., 2020).

[5] Appendix Table A.1 shows that our results are robust to alternative definitions of a relatively frail individual, which we previously define here to be $f \geq h = 0.8$. Specifically, we move the health frail individual cutoff from $h = 0.6$ to $h = 0.85$, recalculating the frail survival rate for all countries and measuring its statistical association with the COVID-19 death rate for each plausible cutoff. Only at $h = 0.85$ do we begin to see decline in the strength of the relationship. This decline is due to a combination of 1) the randomness introduced by the stochastic survival process, 2) the relatively small size of the representative population and, therefore, increasingly frail individuals, and 3) the convergence of the country-specific survival probability functions at the tail of the frailty (age) distribution.

Figure 3: A Simulation of the Longevity-Frailty Hypothesis

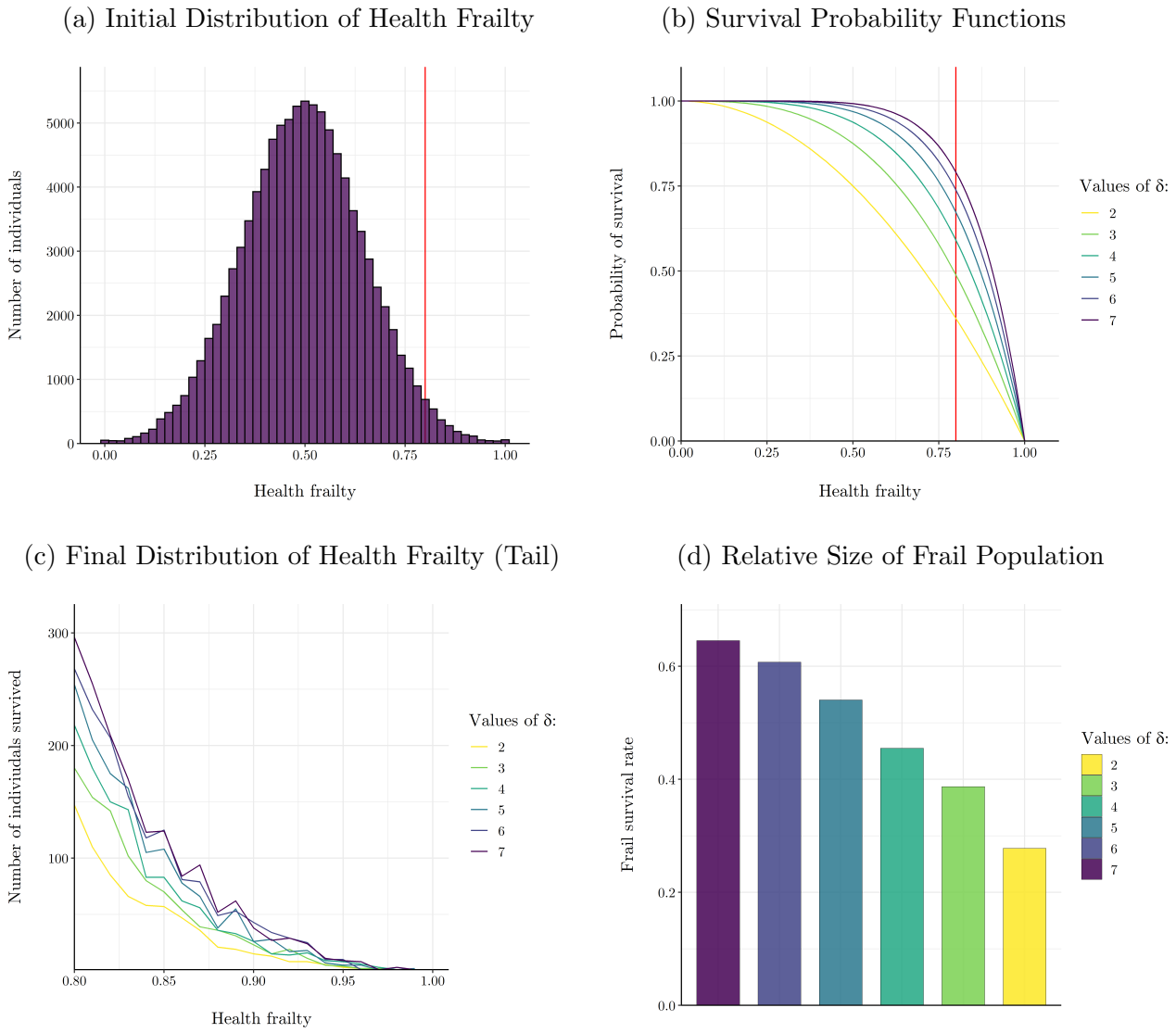

NOTE: Model simulation was performed with R software (version 3.6.1).

The frail survival rate is defined as the number of relatively health frail individuals in period $t = 2$ divided by the number of relatively health frail individuals in period $t = 1$, or

$$\frac{N^2_{f \geq h}}{N^1_{f \geq h}}. \tag{7}$$

From the simulation performed above, one might argue that our simple model supports the use of the elderly population share as an appropriate measure of accumulated health frailty. Specifically, a higher level of total accumulated health frailty and a higher frail survival rate is simply a reflection of a larger number of elderly persons—i.e., number of individuals survived to period $t = 2$. This is certainly true when all countries begin with the same population size in period $t = 1$, but is not the case when countries begin with different population sizes. In Table 1 we perform model simulations for

Table 1: Elderly Population Size and the Rate of Accumulated Health Frailty when Initial Population Sizes Vary

Survival Environment	Size of Initial Population	Size of Elderly Population	Number of Frail Elderly Persons	Frail as % of Elderly Population	Frail Survival Rate
		Simulation A			
$\delta = 5$	100,000	93,591	1,356	1.45	54.0
$\delta = 6$	100,000	95,740	1,524	1.59	60.7
$\delta = 7$	100,000	96,952	1,620	1.67	64.5
		Simulation B			
$\delta = 5$	120,000	112,348	1,606	1.43	53.8
$\delta = 6$	110,000	105,944	1,665	1.58	60.4
$\delta = 7$	100,000	96,952	1,620	1.67	64.5

NOTE: A frail individual is defined by $f \geq h = 0.8$. The size of the elderly population is simply the number of individuals that survive to period $t = 2$. The frail as a percentage of elderly persons is the number of frail persons survived to period $t = 2$ divided by the total number of persons survived to period $t = 2$. The frail survival rate is defined by expression (7).

three hypothetical countries under different assumptions concerning the initial size of each country's population. As previously stated, simulation A shows that the number of persons in period $t = 2$—i.e., the size of the elderly population—can serve as a proxy for differences in accumulated health frailty when the size of the population is identical in the initial period. In simulation B, however, we show that differences in initial population size undermines the size of the elderly population as an effective measure of accumulated health frailty. In particular, the size of the elderly population is larger in countries with a less favorable survival environment, even though rate of frailty accumulation and the frail survival rate is lower. These simulations make clear that elderly population share is a confounded measure of accumulated health frailty. In fact, the COVID-19 death rate and the share of elderly population ≥ 65 are statistically uncorrelated ($r = 0.079$, $p = 0.086$) across the countries of Europe.[6] The frail survival rate, then, provides a more consistent measure of 1) variation in survival environments across countries, 2) the rate of accumulated health frailty, and, therefore, 3) the rate at which an exogenous health shock like COVID-19, which targets the elderly and frail, would operate on a population.

[6]Taking the natural log of both variables still results in statistical independence ($r = 0.061$, $p = 0.752$). Even if one expands the definition of elderly share to persons ≥ 75 years of age, the relationship is statistically insignificant ($r = 0.152$, $p = 0.430$) and only at the share of population ≥ 85 years of age does the relationship to the COVID-19 death rate become moderately correlated and significant ($r = 0.4741$, $p = 0.009$). Percent elderly is an imperfect proxy for elderly survival and consequent frailty accumulation because it is confounded by other components of population size and mortality selection. The numerator of percent elderly partly reflects elderly survival but also reflects other impertinent sources of age structure like the parental fertility of the present elderly relative to the fertility of subsequent cohorts, among other things.

2.2 The Longevity-Frailty Hypothesis Across European Countries

A first step in producing a tangible measure of accumulated health frailty across the countries of Europe is deriving country-specific survival probability functions—i.e. survival environments. Health frailty is unobserved and, therefore, a country's survival probability function can not be derived directly. However, assuming that age provides a sufficient within-country approximation of health frailty—with the young corresponding to least frail and the elderly corresponding to most frail—we employ age-specific probabilities of death to derive survival probability functions across the countries of Europe. In other words, differences in survival environments across European countries will reflect differences in age-specific all-cause mortality rates. Data on age-specific probabilities of death are collected from the Human Mortality Database (HMD) life tables and anchored on the most recently available common year of 2016.

For each European country (j) in our sample we extract the life table component l_x, defined as the number of individuals who survive to age x, which itself is determined by age-specific probabilities of death (q_x). This measure is then transformed as follows

$$p_j(f=0) = 1 - \frac{l^j_{x=0}}{100000}$$
$$\vdots$$
$$p_j(f=1) = 1 - \frac{l^j_{x=110}}{100000}$$

to rest on the domain domain of health frailty $f \in \{0, 0.1, ..., 0.99, 1\}$.[7] The result of this exercise is presented in panel (a) of Figure 4. These country-specific survival probability functions (colored by the size of the area under curve) are, essentially, survivorship curves where the horizontal axis has been transformed to reflect health frailty. While these approximated survival probability functions do not map perfectly to the functional form and conditions derived in the previous section, the consistency of their shape across countries validates their usefulness in measuring relative survival environments for the countries of Europe and allows us to bypass the potentially complicated estimation of δ for each country in our sample.

Using these approximated survival probability functions, we simulate our simple model to produce rates of accumulated health frailty across the countries of Europe. Similar to the previous simulation, each European country in our sample begins in period $t = 1$ with the representative population of 100,000 individuals, each endowed by nature with a level of health frailty (f_i)—see panel (a) of Figure

[7] Given that there are 101 values of f in our discrete model and 110 values of l_x for each country in the HMD, there are some values of health frailty that are assigned two survival probabilities. In these instances we apply the mean of the two probabilities.

Figure 4: Simulating the Longevity-Frailty Hypothesis Across European Countries

(a) Survival Probability Functions

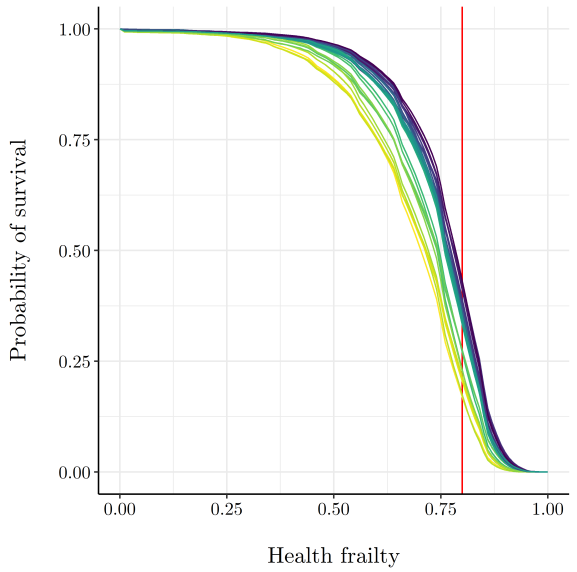

(b) Final Distribution of Health Frailty (Tail)

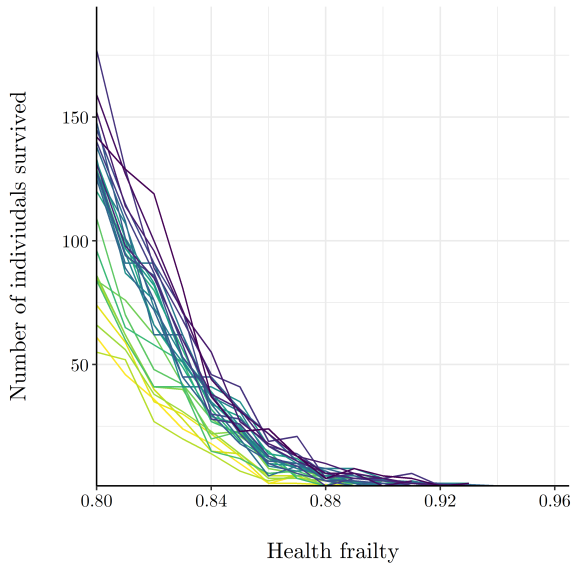

(c) Relative Size of Frail Population

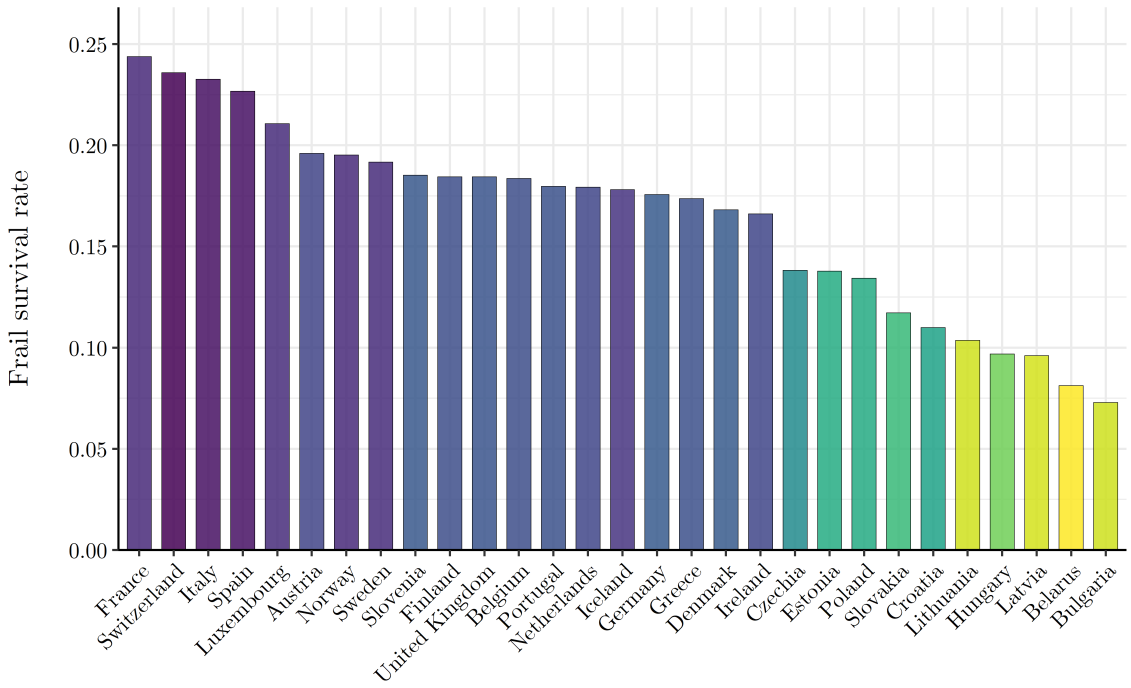

NOTE: The data for each country are colored by the area under the survival curve for all plots. Underlying data for the country-specific survival probability functions shown in panel (a) are from the Human Mortality Database (HMD) life tables and anchored on the most recently available common year of 2016.

3. The stochastic process of survival—repeated Bernoulli trials—is then employed to determine which individuals survive to period $t = 2$. To reiterate this process, consider the marginal health frail individual ($f = h = 0.8$) living in Spain. The approximated survival probability function for Spain determines that likelihood of survival for this individual is $p(0.8) = 0.418$. In other words, this

individual will draw a 0 (dies in period $t = 1$) with probability $1 - p(0.8) = 0.582$ and a 1 (survives to period $t = 2$) with probability $p(0.8) = 0.418$. For a similar individual living in Germany, however, the probability of survival is much lower at $p(0.8) = 0.340$. Again, this Bernoulli trial is performed for each of the 100,000 representative individuals in Spain, Germany, and all other European countries in the sample to arrive at the total number of persons survived to period $t = 2$, or old-age.

The outcome of this stochastic survival process are theoretical distributions of health frailty across the countries of Europe. The tail of these distributions are plotted in panel (b) of Figure 4 where color scheme is maintained from panel (a), reflecting the size of the area under each country's approximated survival probability function. Countries with a more favorable survival environment (purple) have larger populations of health frail individuals in period $t = 2$ relative to countries with a less favorable survival environment (yellow). A summary of these country-specific distributions is presented in panel (c) using the previously defined frail survival rate—expression (7)—where each country, again, is colored by the size of the area under the survival curve. The color ordering in panel (c) is imperfect due to a combination of 1) marginal differences in survival environments, 2) noise introduced by the stochastic survival process, and 3) the relatively small representative population.

One might question the usefulness of using the frail survival rate as the preferred theoretical measure of accumulated health frailty. In particular, the area under each country-specific survival curve for $f \in [h, 1]$, given theoretically by

$$\int_h^1 p(f; \delta) df \tag{8}$$

and practically by

$$\sum_{i=h}^{1} p(f_i) \tag{9}$$

is a similar measure to the frail survival rate that is unbiased by the stochastic survival process. With respect to our statistical analysis and results that follow, both measures behave similarly.[8] However, there are number of arguments that can be made in favor of the frail survival rate as a more robust measure. For instance, administrative differences across countries may produce differences in age-specific probabilities of death that are merely an illusion of reporting heterogeneity. Similarly, some differences in age-specific probabilities of death reported in 2016 may have been period specific and not an indication of real, long-lasting differences in underlying survival environments. Therefore, introducing a small amount randomness through the stochastic survival process is useful in insulating

[8]See Appendix Table A.1.

our results from oddities in the data that are no indication of real differences in underlying survival environments and the accumulation of health frailty across the countries of Europe.

2.3 Validation of the Measures of Relative Health Frailty

Before moving to our investigation of the relationship between accumulated health frailty and COVID-19 mortality across the countries of Europe, we test the validity of our theoretical measures against real measures of late life physiological decline and consequent health frailty. The European Commission, Eurostat database contains information on the 1) percentage of persons ≥ 65 that need help with household activities; 2) percentage of persons ≥ 65 that need help with personal care activities, and 3) percentage of disabled persons ≥ 65 that need the assistance of others. Together, these three variables can form a reasonably good indicator of late life physiological decline requiring the assistance of others and, consequently, health frailty.

Table 2 presents data on these variables for similarly economically developed European countries[9] arranged in descending order on the frail survival rate. In addition to the frail survival rate, we include the frail survival area—the alternative measure of accumulated health frailty discussed in the previous section—to show the similarity between the two measures. Notably, the top 3 countries in terms of longevity score highest on the elderly frailty index, constituting the average of our three indicators of

Table 2: Frail Survival Rates and Indicators of Health Frailty Across European Countries

Country	Frail Survival Rate	Frail Survival Area	% Disabled Need Help	% $\geq$ 65 Need Help Personal Activities	% $\geq$ 65 Need Help House Activities	Health Frailty Index
France	0.244	2.426	54.724	47.033	64.105	55.287
Italy	0.233	2.222	59.906	48.824	54.566	54.432
Spain	0.227	2.325	55.914	55.025	54.033	54.991
Luxembourg	0.211	2.060	32.796	21.290	31.159	28.415
Austria	0.196	1.893	27.164	26.408	23.145	25.572
Norway	0.195	1.999	26.218	23.204	28.316	25.913
Sweden	0.192	1.948	30.734	34.845	37.688	34.422
Finland	0.184	1.809	19.135	24.935	17.969	20.680
United Kingdom	0.184	1.835	46.580	46.122	45.651	46.117
Belgium	0.184	1.887	45.052	42.033	58.718	48.601
Netherlands	0.179	1.739	26.435	26.659	33.776	28.957
Iceland	0.178	1.772	25.556	25.532	25.676	25.588
Germany	0.176	1.710	34.329	31.041	37.655	34.342
Denmark	0.168	1.721	27.530	44.124	30.882	34.179

NOTE: The frail survival rate is drawn from the model simulation presented in panel (c) of Figure 4. The frail survival area is a measure of the area under each country's survival probability function given by expression (9). Elderly frailty data are from The European Commission, Eurostat database. The elderly health frailty index is calculated as the average of the three elderly frailty indicators.

[9] Countries with GDP per capita in 2018 above the median GDP per capita across Europe are included. GDP per capita data are from the World Bank.

assistance need. The correlation between our frailty index and the frail survival rate is positive and statistically significant ($r = 0.631$, $p = 0.016$). The correlation between the frail survival area and the elderly health frailty index is similarly positive and statistically significant ($r = 0.676$, $p = 0.008$).

3 Results

3.1 Country-Specific Survival Environments and COVID-19 Death Rates

In our model we derived a clear relationship between the survival environment and accumulated health frailty—equation (6). With respect to COVID-19 mortality, which disproportionately targets the frail, countries with a more favorable survival environment will have a higher rate of accumulated health frailty and, therefore, a higher COVID-19 death rate. In Figure 5 we replot panel (a) from Figure 4, but with each country's survival probability function now colored by their observed COVID-19 death rate as of May 1st, 2020—yellow reflecting the lowest and purple reflecting the highest.

This striking visualization of COVID-19 death rates across the countries of Europe shows that countries with a relatively unfavorable survival environment—as indicated by a survival probability function bent in towards the origin of the plot—have the lowest observed COVID-19 death rate while the countries with the most favorable survival environments—as indicated by a survival probability

Figure 5: Survival Probability Functions and COVID-19 Death Rates (as of May 1st, 2020)

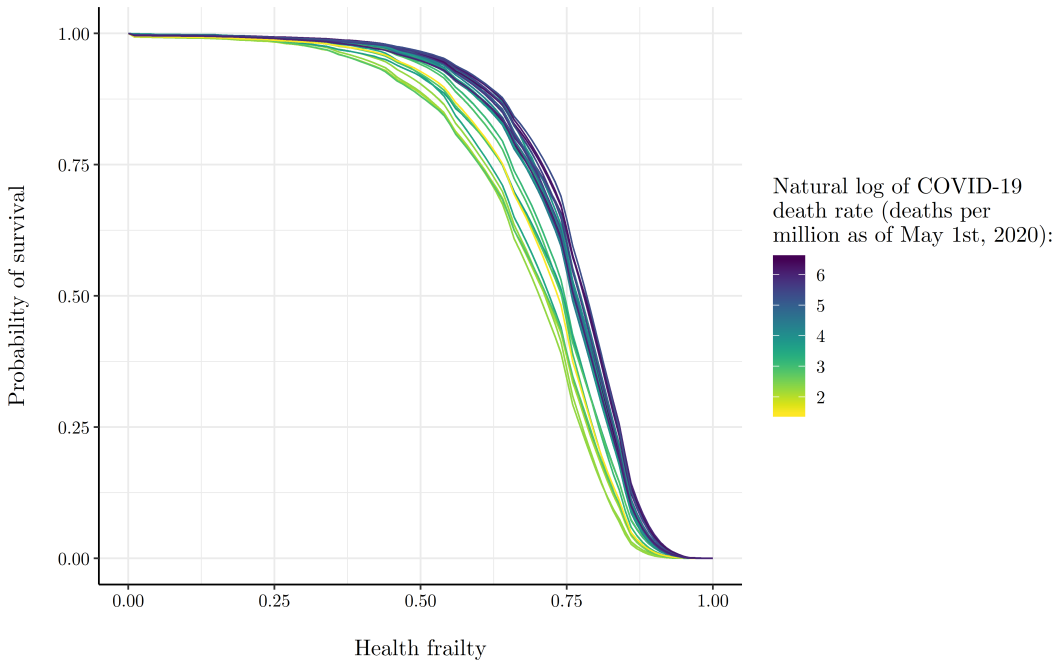

NOTE: COVID-19 death data by country are from Johns Hopkins Coronavirus Resource Center. The underlying data for the country-specific survival probability functions are drawn from the Human Mortality Database (HMD) and anchored on the most recently available common year of 2016.

function bent out and to the right—have the highest observed COVID-19 death rates. This corroborates the implications drawn from our model that a more favorable survival environment leads to higher rates of accumulated health frailty and, therefore, an increased risk of death when confronted with an exogenous health shock that disproportionately targets the health frail.

The country-specific survival probability functions are ultimately derived from age-specific probabilities of death in the HMD. The relationship presented in Figure 5, between the country-specific survival probability functions and the COVID-19 death rate, then suggests an underlying relationship between age-specific all-cause mortality and COVID-19 death rates across the countries of Europe. Higher pre-existing all-cause mortality rates indicate a relatively unfavorable survival environment and lower level of accumulated health frailty. The expectation, then, is that higher pre-existing all-cause mortality will be associated with a lower COVID-19 death rate across the countries of Europe.

The National Institute for Demographic Studies (INED) collects age- and sex-specific COVID-19 death data for select European countries—Denmark, France, Spain, Germany, Italy, the Netherlands, and Spain (Figure 2). We collapse age-specific COVID-19 deaths into common age intervals across the six countries for comparison and calculate corresponding pre-existing all-cause mortality rates using data from the HMD. Age-specific COVID-19 death data is available for all age groups in each country with the exception of the Netherlands, whose data is only available for those 60 years of age and older. Pre-existing all-cause mortality data are collected from the most recently available common year of 2016. To test the statistical relationship between pre-existing all-cause mortality and the COVID-19 death rate, we estimate the following least squares model

$$\ln(CoV_{ij}) = \alpha + \beta \ln(AC_{ij}) + \delta_i + \varepsilon_{ij} \tag{10}$$

where CoV is the COVID-19 death rate for age group i in country j as of May 1st, 2020, AC is the pre-existing all-cause death rate (2016), δ_i is a vector of age-interval fixed effects, and ε is the model disturbance term. Our theoretical interest is in the estimate of β which we expect to be negative, implying, other things equal, a 1% increase in the age-specific all-cause death rate is associated with a β percent decrease in the associated age-specific COVID-19 death rate. We estimate this model for female, male, and total age-specific COVID-19 death rates.

Table 3 reports the coefficient estimates for equation (10). The estimates in columns (1) through (3), when age interval fixed effects are not included in the model, reflect both between- and within-country variation in COVID-19 death rates vis-à-vis pre-existing all-cause mortality rates. In so far as the COVID-19 death rate behaves similarly to that of all other causes of death, intensifying as it moves up the age gradient (Figure 2), there will be a strong positive association between age-specific all-cause

Table 3: Regression Models Predicting Age-Specific Male, Female. and Total COVID-19 Death Rates for Select European Countries

	Female COVID-19 Death Rate (1)	Male COVID-19 Death Rate (2)	Total COVID-19 Death Rate (3)	Female COVID-19 Death Rate (4)	Male COVID-19 Death Rate (5)	Total COVID-19 Death Rate (6)	Female COVID-19 Death Rate (7)	Male COVID-19 Death Rate (8)	Total COVID-19 Death Rate (9)
Female All-Cause Death Rate	1.499***			−3.578**			−2.195**		
	(0.113)			(1.530)			(0.815)		
Male All-Cause Death Rate		1.500***			−3.363**			−5.504***	
		(0.109)			(1.264)			(1.330)	
Total All-Cause Death Rate			1.418***			−2.829**			−4.109***
			(0.093)			(1.243)			(1.054)
10-19 years				−6.394***	−1.516	−2.579*			
				(2.168)	(1.393)	(1.485)			
20-29 years				−1.142	4.365***	2.339***			
				(1.401)	(0.865)	(0.831)			
30-39 years				3.769***	7.014***	4.986***			
				(1.089)	(1.086)	(0.909)			
40-49 years				8.310***	11.060***	8.649***			
				(1.977)	(1.986)	(1.776)			
50-59 years				13.000***	16.005***	12.873***			
				(3.347)	(3.222)	(2.966)			
60-69 years				17.337***	20.278***	16.576***			
				(4.630)	(4.369)	(4.060)			
70-79 years				22.025***	24.500***	20.340***	3.364***	6.100***	4.905***
				(6.067)	(5.463)	(5.153)	(0.857)	(1.211)	(0.992)
80-89 years				27.958***	29.222***	24.692***	7.506***	13.163***	10.734***
				(8.027)	(6.831)	(6.575)	(1.870)	(2.640)	(2.179)
$\geq$ 90 years				33.049***	33.340***	28.474***	10.984***	19.448***	15.889***
				(9.799)	(8.102)	(7.901)	(2.809)	(3.981)	(3.302)
Constant	−9.335***	−9.224***	−8.407***	18.765**	16.952**	14.479*	23.901***	57.452***	42.802***
	(0.954)	(0.964)	(0.805)	(9.017)	(7.669)	(7.441)	(7.195)	(12.565)	(9.675)
Observations	54	54	54	54	54	54	24	24	24
R^2	0.767	0.781	0.814	0.840	0.888	0.890	0.833	0.832	0.836

NOTE: Standard errors in parentheses. Levels of statistical significance are indicated by * $p < 0.1$, ** $p < 0.05$, and *** $p < 0.01$. Reference age interval is 0-9 years for models 1 through 6. Models 7 through 9 restrict to persons 60 years of age and older with the reference age interval being 60-69 years.

and COVID-19 death rates within countries. The positive coefficient estimates in the the first three columns of Table 3, then, indicate that the within-country positive association confounds the expected between-country negative association between pre-existing all-cause mortality and COVID-19 death rates.

In columns (4) through (6) we introduce age interval fixed effects. The inclusion of these variables results in a between-country estimate of β that is purged of the confounding within-country effect of increasing risk of death across age intervals. According to our theoretical expectations, pre-existing all-cause mortality rates are estimated to have a strong, negative association with the COVID-19 death rate across countries. The coefficient estimate of -3.578 for females in column (4) implies that, other things equal, a 1% decrease in the pre-existing all-cause death rate is associated with an approximate 3.6 percent higher COVID-19 death rate, on average across age intervals. The coefficient is similarly large (-3.363) and statistically significant for males—shown in column (5)—and for the total death rate (-2.829)—column (6). In the final three columns of the table we reduce the sample to ≥ 60 years of age. The qualitative nature of the estimates are maintained, though the negative association between pre-existing all-cause mortality and the COVID-19 death rate appears to be stronger for males than females among the elderly. Specifically, a 1% decrease in the pre-existing all-cause death rate is associated with an approximate 4.1 percent increase in the total COVID-19 death rate for those ≥ 60 years of age, other things equal.

3.2 Accumulated Health Frailty and COVID-19 Death Rates

In this section we investigate the relationship between our model-generated measure of accumulated health frailty—the frail survival rate shown in panel (c) of Figure 4—and the COVID-19 death rate. In Figure 6, countries are colored by their frail survival rate, with yellow reflecting the lowest and purple reflecting the highest. The natural log of the COVID-19 death rate is manifestly upward sloping in our measure of accumulated health frailty. The positive statistical relationship is strong ($r = 0.772$, $p < .001$) and indicates that a higher level of accumulated health frailty predicts a higher COVID-19 death rate.

Next, we test if the relationship between accumulated health frailty and COVID-19 death rates presented in Figure 6 is robust to the inclusion of variables that operationalize other candidate hypotheses, namely healthcare capacity (Verhagen et al., 2020), seeding from international tourists, as well as the timing and stringency of non-pharmaceutical interventions (NPI) (Pan eat al., 2020). We collected data from the World Bank on hospital beds per 1,000 persons (2015/2016) and the annual

Figure 6: COVID-19 Death Rates (as of May 1st, 2020) and Health Frailty

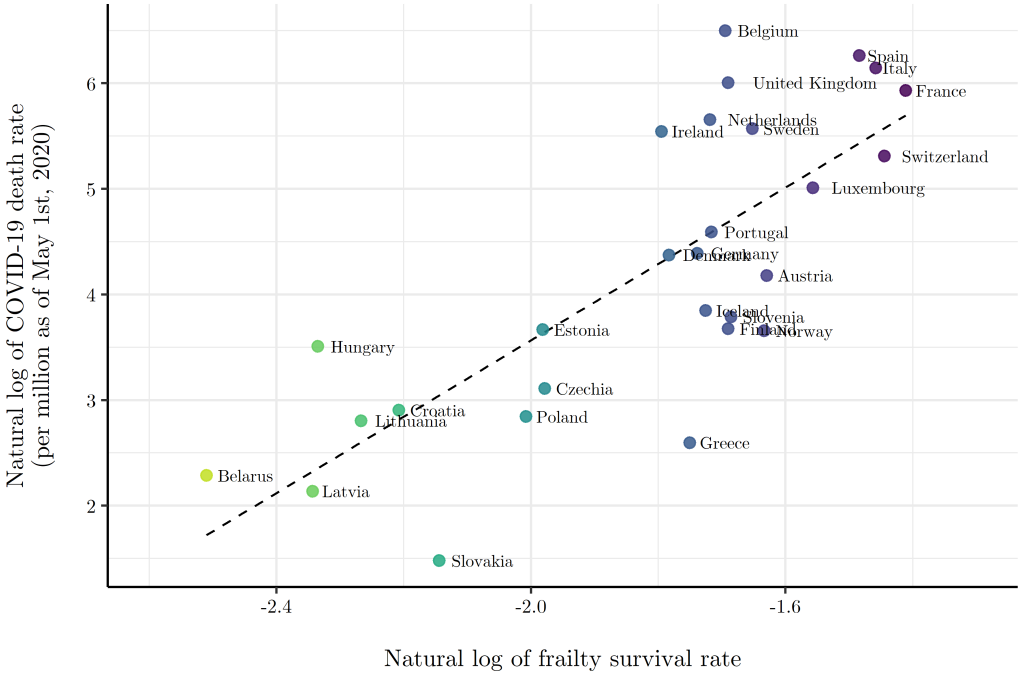

NOTE: COVID-19 death data by country are from Johns Hopkins Coronavirus Resource Center. The frailty survival rate is the result of the model simulation presented in Figure 4.

count of inbound international tourists (2018).[10] Data on NPI timing and stringency is collected from the Oxford COVID-19 Government Response Tracker (Hale et al., 2020). The NPI timing variable is time-invariant and measured in relation to the day of the first reported COVID-19 death(s). Specifically, we measure the daily distance between the first reported COVID-19 death and five separate initial policy responses—school closures, workplace closures, the cancellation of public events, restrictions on gatherings, and stay at home orders. The final NPI timing variable constitutes the average policy timing across the five individual measures—negative and positive values reflect proactive and reactive policies, respectively. The policy stringency measure is time-variant index calculated according to the work of Hale et al. (2020), ranging from 0 (least stringent) to 100 (most stringent). Recent research suggests that the the lag between when transmission changes occur and when their impact can be observed in trends in mortality is 2-3 weeks (Flaxman et al., 2020). We lag our measure of NPI stringency by 2.5 weeks.[11]

[10] According to World Bank documentation, the hospital beds per 1,000 includes: "Hospital beds include inpatient beds available in public, private, general, and specialized hospitals and rehabilitation centers. In most cases beds for both acute and chronic care are included." With respect to international tourist counts, the World Bank notes: "International inbound tourists (overnight visitors) are the number of tourists who travel to a country other than that in which they have their usual residence, but outside their usual environment, for a period not exceeding 12 months and whose main purpose in visiting is other than an activity remunerated from within the country visited. The data on inbound tourists refer to the number of arrivals, not to the number of people traveling. Thus, a person who makes several trips to a country during a given period is counted each time as a new arrival."

[11] We tested multiple lag structures for policy stringency—from 1 week to 4 weeks. Our results are robust to these alternative lag structures.

Due to the time-invariant nature of our covariates of interest, as well as the cross-sectional, time-series nature of the data, we estimate versions of the following random effects model with an autoregressive disturbance structure:

$$\ln(CoV_{jt}) = \alpha + \beta \ln(FSR_j) + \Gamma_1 \ln(H_j) + \Gamma_2 \ln(IT_j) + \Gamma_3 PT_j + \Gamma_4 \ln(PS_{jt}) + T_{jt} + \delta_t + \nu_j + \epsilon_{jt} \tag{11}$$

where

$$\epsilon_{jt} = \rho \epsilon_{jt-1} + \eta_{jt}. \tag{12}$$

CoV is either the cumulative or weekly reported COVID-19 death rate for country j in week t, FSR is the model generated frail survival rate (which rests on 2016 age-specific probabilities of death from the HMD), H is hospital beds per 1,000 persons in 2015/2016, IT is the count of international inbound arrivals to a country in 2018, PT is our metric of overall NPI timing measured in days since the first reported COVID-19 death(s), and PS is overall policy response stringency. ν_j is a country-specific random effect and ϵ_{jt} is the model disturbance term which is assumed to follow the AR(1) process described by equation (12)—where $|\rho| < 1$ and η_{jt} is independent and identically distributed (i.i.d.) with mean 0 and variance σ^2_η.

Week is defined according to both calendar time and epidemic time, with models being estimated for each definition. When the unit of analysis is defined according to the calendar week, δ is a vector of calendar week fixed effects and T is a continuous variable for epidemic time—measured as days since the first reported death(s). Here, we collect data from the most recently available date (May 1, 2020 at the time of analysis) and move backwards in 7 day increments for 6 weeks to build the panel of data across the countries of Europe. Oppositely, when the unit of analysis is defined according to epidemic week, δ is a vector of epidemic week fixed effects and T is a continuous variable of calendar time—measured in days. Epidemic time starts on the day of the first reported COVID-19 death for each country and we collect data in seven day increments, moving forward through epidemic time, to build this alternative panel of data.

Our theoretical interest is the relationship between accumulated health frailty and the COVID-19 death rate, which we have previously shown to be positive. Thus, the estimate of β is expected to be positive, meaning a 1% increase the the frail survival rate will be associated with a β percent increase in the COVID-19 death rate. The necessary assumption for the identification of β is $E[\nu_j|FSR_j] = 0$, with a similar condition being required for the identification of the coefficients on the other covariates.

In other words, ν_j are assumed to be realizations of an i.i.d. process with mean 0 and variance σ_ν^2. We report the correlation between the model estimated random effects ($\hat{\nu}$) and our variable of interest (FSR) in our results.

Table 4 reports the coefficient of interest for our random effects regression model under alternative definitions of the COVID-19 death rate and time.[12] Columns (1) through (3) present estimates from the random effects model when the COVID-19 death rate is defined to be cumulative, while columns (4) through (6) correspond to the weekly COVID-19 death rate. Further, Panel A present the model estimates when time is defined according to the calendar week and Panel B presents the model estimates under the epidemic week definition of time. Beginning in column (1) of Panel A we find that the positive association between the frail survival rate and the cumulative COVID-19 death rate is robust to the control of competing hypotheses. The statistically significant coefficient estimate of 2.627 implies that a 1% increase in accumulated health frailty, as measured through the frail survival rate, is associated with an approximate 2.6 percent increase in the cumulative COVID-19 death rate, all else constant. The policy response data is unavailable for three European countries in our sample—Belarus, Latvia, and Lithuania. Therefore, in column (2) we reduce our sample to only those countries for which policy data is available and then introduce policy response variables in column (3) for compositional similarity. Removing Belarus, Latvia, and Lithuania in column (2) marginally increases the coefficient estimate on the frail survival rate and this estimate is effectively invariant to the inclusion of policy controls in column (3).

In columns (4) through (6) of panel A we observe that the estimated relationship is not dependent on the cumulative definition of the COVID-19 death rate. Specifically, when the dependent variable is defined to be the weekly COVID-19 death rate, a 1% increase in the frail survival rate is associated with an approximate 2.2 percent increase in the COVID-19 death rate. This estimate is also robust to the sample reduction and inclusion of policy controls in columns (2) and (3), respectively. The estimate of ρ is reported for all models in Table 4 along with the associated modified Bhargava et al. (1982) Durbin-Watson and Baltagi-Wu (1999) locally best invariant (LBI) test statistics under the null hypothesis $\rho = 0$. This null hypothesis is rejected across all models presented in Table 4 and implies that the modeled AR(1) disturbance structure appropriately corrects the model estimated standard errors.

In Panel B, the estimated coefficient on the frail survival rate decreases relative to the estimates produced by the models in Panel A, though they remain statistically significant and continue to out perform the coefficient estimates associated with alternative hypotheses.[13] To reiterate, time is

[12] Appendix Table A.2 reports coefficient estimates for the full model.
[13] See Appendix Table A.2.

Table 4: Random Effects Regression Models Predicting
Cumulative and Weekly COVID-19 Deaths

	Dependent Variable: Natural Log Cumulative COVID-19 Death Rate			*Dependent Variable:* Natural Log Weekly COVID-19 Death Rate		
	(1)	(2)	(3)	(4)	(5)	(6)
Panel A: Unit of Analysis is Date Time (Weekly) (Calendar week FEs included in all models)						
Natural Log Frail Survival Rate	2.627***	2.822***	2.846***	2.202***	2.287***	2.342***
	(0.681)	(0.715)	(0.708)	(0.752)	-0.805	-0.788
Observations	172	155	155	144	129	129
R^2	0.79	0.77	0.77	0.61	0.55	0.55
$\hat{\rho}$	0.364	0.428	0.388	0.266	0.283	0.274
Bhargrva et al. Durbin-Watson	0.573	0.473	0.679	0.841	0.829	0.866
Baltagi-Wu LBI	1.275	1.143	1.293	1.469	1.435	1.459
$Cor(\hat{u}, FSR)$	-0.155	-0.128	-0.105	-0.148	-0.116	-0.102
p-value	0.421	0.533	0.608	0.453	0.580	0.628
Panel B: Unit of Analysis is Epidemic Time (Weekly) (Epidemic week FEs included in all models)						
Natural Log Frail Survival Rate	2.022***	2.639***	2.658***	2.178***	2.372***	2.398***
	-0.607	-0.697	-0.712	-0.651	-0.733	-0.757
Observations	215	171	171	180	157	157
R^2	0.8	0.8	0.8	0.58	0.56	0.57
$\hat{\rho}$	0.526	0.51	0.504	0.431	0.458	0.42
Bhargrva et al. Durbin-Watson	0.426	0.487	0.532	0.491	0.446	0.588
Baltagi-Wu LBI	0.959	1.024	1.061	1.145	1.089	1.241
$Cor(\hat{u}, FSR)$	0.300	0.252	0.252	0.305	0.054	0.035
p-value	0.114	0.298	0.298	0.139	0.845	0.900
Controls	X	X	X	X	X	X
Reduced policy sample		X	X		X	X
Policy controls			X			X

NOTE: Standard errors in parentheses. Levels of statistical significance are indicated by * $p < 0.1$, ** $p < 0.05$, and *** $p < 0.01$. All models incorporate an AR(1) error structure and the estimated ρ is reported along with the associated modified Bhargava et al. Durbin-Watson and Baltagi-Wu locally best invariant (LBI) test statistics, both of which have complicated distributions (Bhargava et al., 1982; Baltagi & Wu, 1999). In all cases we reject the null hypothesis of $\rho = 0$.

defined according to calendar week in Panel A and epidemic week in Panel B. Now, other things equal, a 1% increase in the frail survival rate is associated with a 2.02 percent increase in the cumulative COVID-19 death rate. Similar to Panel A, removing Belarus, Latvia, and Lithuania—countries with missing NPI data—from the sample increases the size of the estimated coefficient in column (2) and this coefficient estimate is effectively unchanged upon the inclusion of policy controls in column (3). Mirroring the estimates reported in Panel A, columns (4) through (6) of panel B indicate that the estimated relationship between accumulated health frailty and COVID-19 mortality is not dependent on the cumulative definition of the COVID-19 death rate.[14]

From the results reported in Table 4 we conclude that a 1% increase in the rate of accumulated health frailty is associated with a 2-2.6 percent increase in the COVID-19 death rate, other things equal, across the countries of Europe. For reference, a movement in the frail survival rate from the 50th (Iceland) to 75th (Sweden) percentile, representing a 7.6% increase in the frail survival rate, corresponds to an approximate 15-20 percent increase in the COVID-19 death rate, other things equal. Alternatively, a movement in the frail survival rate from the 25th (Poland) to 75th (Sweden) percentile represents a 42.7% increase in the frail survival rate and an approximate 85-111 percent increase in the COVID-19 death rate.

4 Conclusion

In this paper we developed measures of accumulated health frailty in an attempt to explain observed differences in COVID-19 mortality across the countries of Europe. We began by developing a simple model of longevity and accumulated health frailty, where heterogeneous survival environments across countries induce a mortality selection process that generates varying amounts of accumulated health frailty in subsequent periods, or old-age. Using pre-existing age-specific probabilities of death and our model-generated measures of accumulated health frailty, we link cross-national variation in survival environments and consequent accumulated health frailty to the puzzling distribution of COVID-19 death rates in Europe.

We find that a more favorable survival environment, as indicated by lower pre-existing all-cause mortality rates, is positively associated with COVID-19 death rates. Specifically, a 1% decrease in pre-existing all-cause mortality is associated with a 2.8 percent increase in the COVID-19 death rate,

[14] To reiterate the confounded nature of percent elderly as an effective measure of accumulated health frailty we reestimate the models of Table 4, replacing the frail survival rate with elderly population shares—e.g. percent of the population $\geq$ 65, 70, 75, 80, 85, and 90 years of age. The results are presented in Appendix Table A.3. The share of the population $\geq$ 90 years of age behaves most similarly, though imperfectly, when compared to our model-generated measure of accumulated health frailty. This is expected since the share of the population $\geq$ 90 years of age is a less confounded measure of longevity, largely reflecting differences in survival environments and the consequent accumulation of health frailty across countries.

on average, for all age groups and a 4.1 percent increase in the COVID-19 death rate, on average, for those ≥ 60 years of age. COVID-19 death rates are also positively associated with our model-generated measures of accumulated health frailty ($r = 0.772$, $p < .001$). Importantly, this relationship is robust to statistical control for the timing and strength of epidemic seeding from exported cases, the capacity of a healthcare system to manage and survive infected persons, as well as the timing and stringency of non-pharmaceutical interventions.

Our results oblige the widely observed facts that the risk of COVID-19 mortality is nonlinearly increasing in age and that a disproportionate share of deaths are occurring among frail populations. Specifically, data show that a large percentage of COVID-19 deaths are occurring in nursing homes—Belgium (53%), Denmark (34%), France (51%), Germany (36%), Hungary (19%), Ireland (60%), Norway (60%), Portugal (40%), and Sweden (45%).[15] Recent reports on the share of COVID-19 deaths occurring in long-term care facilities in the United States (35%)[16] and Canada (81%)[17] suggest that this phenomena generalizes beyond the countries of Europe. In France, Spain and Italy, among the hardest hit countries of Europe, about half to two-thirds of elderly require assistance for basic personal and household care activities. This fact educates that a sizeable percentage of European elderly cannot easily socially distance, compounding the risk of COVID-19 mortality.

Moreover, viral spread through the social intimacy that characterizes elderly care is plausibly associated with a higher viral load of initial infection as compared with random contact, a factor implicated in disease severity (Liu et al, 2020). Several other characteristics of SARS-Cov2 are relevant to the problem of high mortality risk among the elderly of Europe. First, several studies have shown that the elderly are particularly susceptible to this virus for reasons that are not yet fully understood (Verity et al, 2020, Liu et al, 2020, Huang et al, 2020). Second, a significant percentage of infected persons are asymptomatic (estimates range from 15% - 50%), and asymptomatic persons can shed viruses and infect others (Verity et al, 2020). Also, a large percentage of symptomatic patients exhibit mild symptoms that can be confused with a more common cold or flu. Third, viral replication has been shown to be highest in the early days of infection, when most people are mildly or asymptomatic (Zhou, Fei et al, 2020). Thus, in the context of caregiving, people with little or no symptoms can be potent spreaders of the virus to the susceptible elderly and frail. The many stories of outbreak and death in nursing homes testifies to this transmission channel. This necessitates more intense testing

[15] These data come from the International Long-Term Care Policy Network (Comas-Herrera et al., 2020) (https://ltccovid.org/wp-content/uploads/2020/05/Mortality-associated-with-COVID-3-May-final-5.pdf) and Sciensano, a public research institution which publishes very detailed epidemiological daily reports on COVID-19 (https://covid-19.sciensano.be/sites/default/files/Covid19/covid-19_daily_report_20200505_-_fr.pdf).

[16] https://www.nytimes.com/interactive/2020/05/09/us/coronavirus-cases-nursing-homes-us.html

[17] https://www.washingtonpost.com/world/the_americas/coronavirus-canada-long-term-care-nursing-homes/2020/05/18/01494ad4-947f-11ea-87a3-22d324235636_story.html

of caregivers to break transmission to the elderly and frail.

References

Almond, D. & Currie, J. (2011). Killing Me Softly: The Fetal Origins Hypothesis. *The Journal of Economic Perspectives. 25*(3): 153–172. doi:10.1257/jep.25.3.153.

Baltagi, B. H., P. X. Wu. (1999). Unequally spaced panel data regressions with AR(1) disturbances. *Econometric Theory.* 15: 814–823.

Bhargava, A., L. Franzini, W. Narendranathan. (1982). Serial correlation and the fixed effects model. *Review of Economic Studies.* 49: 533–549.

The Demographics of COVID-19 Deaths (2020). National Institute for Demographic Studies (INED). Extract from: https://dc-covid.site.ined.fr/en/ (02/05/2020).

Denfeld QE, Winters-Stone K, Mudd JO, Gelow JM, Kurdi S, Lee CS. The prevalence of frailty in heart failure: A systematic review and meta-analysis. Int J Cardiol. 2017 Jun 1; 236:283-289

Dowd, JB., Rotondi V, Adriano L, Brazel DM, Block P, Ding X, Liu Y and Mills MC (2020). Demographic science aids in understanding the spread and fatality rates of COVID-19. *Proceedings of the National Academy of Sciences*, *117*(18): 9696-9698.

C. Dudel, T. Riffe, M. Myrskyla, A. van Raalte, E. Acosta. (2020). Monitoring trends and differences in COVID-19 case fatality rates using decomposition methods: Contributions of age structure and age-specific fatality. medRxiv, 10.31235/osf.io/j4a3d.

Hale, Thomas, Sam Webster, Anna Petherick, Toby Phillips, and Beatriz Kira (2020). Oxford COVID-19 Government Response Tracker, Blavatnik School of Government. Data use policy: Creative Commons Attribution CC BY standard.

Instituto Superiore di Sanità. Characteristics of COVID-19 patients dying in Italy Report based on available data on April 9th. 2020.

Hoogendijk EO, Afilalo J, Ensrud KE, Kowal P, Onder G, Fried LP. Frailty: implications for clinical practice and public health. Lancet. 2019 Oct 12; 394(10206):1365-1375.

Huang C Wang Y Li X et al. Clinical features of patients infected with 2019 novel coronavirus in Wuhan, China. Lancet. 2020; 395:497-506.

A. Pan et al., (2020) Association of public health interventions with the epidemiology of the COVID-19 outbreak in Wuhan, China. *JAMA*, *323*(19): 1915-1923.

Theou O, Squires E, Mallery K, Lee JS, Fay S, Goldstein J, Armstrong JJ, Rockwood K. What do we know about frailty in the acute care setting? A scoping review. BMC Geriatr. 2018 Jun 11; 18(1):139.

M. D. Verhagen, D. M. Brazel, J. B. Dowd, I. Kashnitsky, M. C. Mills. (2020). Predicting peak hospital demand: Demographics, spatial variation, and the risk of hospital deserts during COVID-19 in England and Wales. OSF, 10.31219/osf.io/g8s96.

Vaupel JW, Manton KG, Stallard E. The impact of heterogeneity in individual frailty on the dynamics of mortality. Demography. 1979 Aug; 16(3):439-54.

Verity R, Okell LC, Dorigatti I, et al. Estimates of the severity of coronavirus disease 2019: a model-based analysis. Lancet Infect Dis. 2020; Mar 30.

Vetrano DL, Palmer KM, Galluzzo L, Giampaoli S, Marengoni A, Bernabei R, Onder G; Joint Action ADVANTAGE WP4 group. Hypertension and frailty: a systematic review and meta-analysis. BMJ Open. 2018 Dec 28; 8(12).

Vogt TC and Missov TI. Estimating the contribution of mortality selection to the East–West German mortality convergence. Popul Health Metr. 2017; 15: 33.

Yancy CW. COVID-19 and African Americans. *JAMA*. Published online April 15, 2020. doi:10.1001/jama.2020.654

Yang L, Li-Meng Y, Lagen W, Tian-Xin X, Aiping L, Jia-Ming L, et al. Viral dynamics in mild and severe cases of COVID-19. Lancet Infect Dis. 2020; Mar 19.

Zhonghua L, Xing Bing X, Za Z. The epidemiological characteristics of an outbreak of 2019 novel coronavirus diseases (COVID-19) in China. Novel Coronavirus Pneumonia Emergency Response Epidemiology Team. 2020; 41 (in Chinese): 145-151.

Zhou F, Yu T, Du R, Fan G, Liu Y, Liu Z, Xiang J, Wang Y, Song B, Gu X, Guan L. Clinical course and risk factors for mortality of adult inpatients with COVID-19 in Wuhan, China: a retrospective cohort study. Lancet. 2020 Mar 11.

Appendix

Table A.1: Correlations Between Accumulated Health Frailty and the COVID-19 Death Rate (as of May 1st, 2020) and Under Alternative Health Frailty Cutoffs

Frail Cutoff ($f \geq h$)	Correlation Between Natural Log Frail Survival Rate and Natural Log COVID-19 Death Rate	Correlation Between Natural Log Frail Survival Area and Natural Log COVID-19 Death Rate
0.60	0.745***	0.769***
0.65	0.752***	0.773***
0.70	0.763***	0.777***
0.75	0.767***	0.781***
0.80	0.772***	0.783***
0.85	0.677***	0.775***

NOTE: All correlations are statistically significant with $p < 0.001$ (***). The frail survival rate and the frail survival area are defined by expressions (7) and (9), respectively. COVID-19 death data by country are from Johns Hopkins Coronavirus Resource Center.

Table A.2: Estimated Coefficients for All Covariates in Table 4 Models

	Dependent Variable: Natural Log Cumulative COVID-19 Death Rate			*Dependent Variable:* Natural Log Weekly COVID-19 Death Rate		
	(1)	(2)	(3)	(4)	(5)	(6)
Panel A: Unit of Analysis is Date Time (Weekly) (Calendar week FEs included in all models)						
Natural Log Frail Survival Rate	2.627***	2.822***	2.846***	2.202***	2.287***	2.342***
	(0.681)	(0.715)	(0.708)	(0.752)	-0.805	-0.788
Natural Log Hospital Beds	-0.747	-0.979*	-0.884	-0.571	-0.743	-0.552
	(0.551)	(0.589)	(0.634)	(0.608)	(0.663)	(0.707)
Natrual Log International Arrivals	0.0735	0.0325	0.0367	0.179	0.135	0.16
	(0.179)	(0.197)	(0.195)	(0.198)	(0.222)	(0.217)
Epidemic Time (Days since first death)	0.0487*	0.0577*	0.0413	0.0316	0.0426	0.0165
	(0.027)	(0.030)	(0.034)	(0.030)	(0.034)	(0.038)
Policy Timing (Days from first death)			0.0201			0.0349
			(0.024)			(0.027)
Natural Log Policy Stringency			0.499***			0.605**
			(0.122)			(0.259)
Observations	172	155	155	144	129	129
R^2	0.79	0.77	0.77	0.61	0.55	0.55
Panel B: Unit of Analysis is Epidemic Time (Weekly) (Epidemic week FEs included in all models)						
Natural Log Frail Survival Rate	2.022***	2.639***	2.658***	2.178***	2.372***	2.398***
	(0.607)	(0.697)	(0.712)	(0.651)	(0.733)	(0.757)
Natural Log Hospital Beds	-0.809*	-1.090*	-1.084*	-0.960*	-1.250**	-1.312**
	(0.492)	(0.564)	(0.621)	(0.527)	(0.591)	(0.661)
Natural Log International Arrivals	-0.19	-0.0636	-0.0564	0.101	0.0738	0.076
	(0.161)	(0.190)	(0.194)	(0.173)	(0.200)	(0.207)
Time (Days)	0.0565**	0.0679**	0.0672**	0.0538**	0.046	0.0367
	(0.024)	(0.029)	(0.034)	(0.026)	(0.031)	(0.036)
Policy Timing (Days from first death)			0.00585			0.00662
			(0.024)			(0.026)
Natural Log Policy Stringency			0.218			0.516***
			(0.159)			(0.196)
Observations	215	171	171	180	157	157
R^2	0.8	0.8	0.8	0.58	0.56	0.57
Controls	X	X	X	X	X	X
Reduced Policy Sample		X	X		X	X
Policy Controls			X			X
AR(1) Model	X	X	X	X	X	X

NOTE: Standard errors in parentheses. Levels of statistical significance are indicated by * $p < 0.1$, ** $p < 0.05$, and *** $p < 0.01$. Though not reported, we test an alternative inclusion of the epidemic time trend as the country-specific mean ($\bar{T}_j$) along with the mean difference ($T_{jt} - \bar{T}_j$). This decomposes the epidemic time trend estimate into its within and between components. We find that the coefficient estimate is largely driven by between-country variation, which is somewhat expected given that a substantial of portion within-country variation over time is accounted for through the week fixed effects. We perform a similar exercise for the time-variant measure of policy stringency and find that the coefficient estimate is determined, almost entirely, by within-country variation. This coefficient estimate may be reflecting endogenous policy intervention—i.e. countries ramp up their policy response as their death toll begins to rise. We speculate here, however, a robust analysis of the effect of non-pharmaceutical interventions on the COVID-19 death rate is beyond the scope of this paper.

Table A.3: Random Effects Regression Models Testing the Replacement of the Frail Survival Rate with Measures of Percent Elderly

	Dependent Variable: Natural Log Cumulative COVID-19 Death Rate			*Dependent Variable:* Natural Log Weekly COVID-19 Death Rate		
	(1)	(2)	(3)	(4)	(5)	(6)
Panel A: Unit of Analysis is Date Time (Weekly) (Calendar week FEs included in all models)						
(Each cell represents a unique regression)						
Natural Log Percent Pop. > 65 yrs	-1.365	-1.277	-0.85	-1.238	-1.097	-0.0144
	(1.536)	(1.868)	(2.022)	(1.566)	(1.918)	(2.032)
Natural Log Percent Pop. > 70 yrs	-0.199	0.167	0.701	-0.299	0.0699	1.092
	(1.318)	(1.636)	(1.741)	(1.340)	(1.676)	(1.730)
Natural Log Percent Pop. > 75 yrs	0.214	0.506	0.915	-0.0366	0.254	0.993
	(1.099)	(1.336)	(1.401)	(1.120)	(1.371)	(1.393)
Natural Log Percent Pop. > 80 yrs	0.565	0.857	1.150	0.240	0.532	1.052
	(1.034)	(1.226)	(1.257)	(1.058)	(1.264)	(1.254)
Natural Log Percent Pop. > 85 yrs	1.335	1.714	1.900*	0.888	1.232	1.548
	(0.960)	(1.097)	(1.097)	(0.998)	(1.152)	(1.113)
Natural Log Percent Pop. > 90 yrs	1.748**	2.030**	2.090**	1.374*	1.624*	1.727*
	(0.784)	(0.861)	(0.855)	(0.829)	(0.920)	(0.882)
Observations	172	156	156	144	129	129
Panel B: Unit of Analysis is Epidemic Time (Weekly) (Epidemic week FEs included in all models)						
(Each cell represents a unique regression)						
Natural Log Percent Pop. > 65 yrs	-1.500	-1.377	-1.342	-1.176	-0.776	0.202
	(1.310)	(1.581)	(1.814)	(1.416)	(1.709)	(1.869)
Natural Log Percent Pop. >70 yrs	-0.428	-0.0505	0.175	-0.210	0.405	1.310
	(1.133)	(1.394)	(1.578)	(1.218)	(1.493)	(1.595)
Natural Log Percent Pop. > 75 yrs	0.0471	0.421	0.521	0.189	0.690	1.118
	(0.946)	(1.140)	(1.277)	(1.016)	(1.221)	(1.289)
Natural Log Percent Pop. > 80 yrs	0.345	0.714	0.778	0.433	0.885	1.129
	(0.892)	(1.048)	(1.149)	(0.959)	(1.125)	(1.164)
Natural Log Percent Pop. > 85 yrs	0.954	1.363	1.428	1.035	1.508	1.711*
	(0.834)	(0.944)	(1.014)	(0.902)	(1.019)	(1.028)
Natural Log Percent Pop. > 90 yrs	1.242*	1.524**	1.575**	1.370*	1.701**	1.866**
	(0.692)	(0.755)	(0.803)	(0.750)	(0.815)	(0.808)
Observations	215	198	198	180	166	166
Controls	X	X	X	X	X	X
Reduced Policy Sample		X	X		X	X
Policy Controls			X			X
AR(1) Model	X	X	X	X	X	X

NOTE: Standard errors in parentheses. Levels of statistical significance are indicated by * $p < 0.1$, ** $p < 0.05$, and *** $p < 0.01$. The models reported in the table above are identical to the models reported in Tables 4 and A.2, with the exception being that the frail survival rate is replaced with measures of percent elderly.